

NIST Technical Note 1970

Measurement Uncertainty in the Hydronic System in the IBAL

Dr. Amanda J. Pertzborn

This publication is available free of charge from:
<https://doi.org/10.6028/NIST.TN.1970>

NIST
**National Institute of
Standards and Technology**
U.S. Department of Commerce

NIST Technical Note 1970

Measurement Uncertainty in the Hydronic System in the IBAL

Dr. Amanda J. Pertzborn
*Energy and Environment Division
Engineering Laboratory*

This publication is available free of charge from:
<https://doi.org/10.6028/NIST.TN.1970>

September 2017



U.S. Department of Commerce
Wilbur L. Ross, Jr., Secretary

National Institute of Standards and Technology
Kent Rochford, Acting NIST Director and Under Secretary of Commerce for Standards and Technology

Certain commercial entities, equipment, or materials may be identified in this document in order to describe an experimental procedure or concept adequately. Such identification is not intended to imply recommendation or endorsement by the National Institute of Standards and Technology, nor is it intended to imply that the entities, materials, or equipment are necessarily the best available for the purpose.

**National Institute of Standards and Technology Technical Note 1970
Natl. Inst. Stand. Technol. Tech. Note 1970, 39 pages (September 2017)
CODEN: NTNOEF**

**This publication is available free of charge from:
<https://doi.org/10.6028/NIST.TN.1970>**

Abstract

The Intelligent Building Agents Laboratory (IBAL) has been designed and constructed to demonstrate the potential for distributed, intelligent software agents to perform optimization of control systems in commercial buildings. This technical note discusses the methods used to assess the time-dependent variability of measurement devices in the hydronic system of the IBAL. The total uncertainty is calculated by combining this variability with the uncertainty of the instrumentation.

Acknowledgements

I would like to recognize Dr. James Yen of the Statistical Engineering Division at NIST for his consultation on the statistical analysis used in this report.

TABLE OF CONTENTS

Abstract.....	i
Acknowledgements.....	ii
TABLE OF FIGURES.....	iv
TABLE OF TABLES.....	v
Nomenclature.....	vi
1. Introduction.....	1
2. Uncertainty Calculations.....	3
2.1. Time-Dependent Variability.....	3
2.2. Uncertainty of the Calibration Curve Fit [1].....	5
2.3. Uncertainty of Data Acquisition Equipment.....	6
2.4. Combining Uncertainties.....	8
3. Experimental Design.....	9
3.1. Pump Test Matrices.....	9
3.2. Valve Test Matrices.....	11
3.3. Complete Test Plan.....	12
4. Results.....	12
4.1. Pumps.....	12
4.1.1. Results.....	12
4.1.2. Summary.....	23
4.2. Valves.....	25
4.2.1. Results.....	26
4.2.2. Summary.....	29
5. Conclusions.....	29
6. References.....	30

TABLE OF FIGURES

Figure 1. Schematic of the IBAL. HX3 is the water side economizer.....	2
Figure 2. Results for Pump 1.	13
Figure 3. Total uncertainty of Pump 1.	14
Figure 4. Time-dependent variability versus instrument uncertainty for Pump 1.	15
Figure 5. Results for Pump 2.	16
Figure 6. Total uncertainty of Pump 2.	16
Figure 7. Time-dependent variability versus instrument uncertainty for Pump 2.	17
Figure 8. Results for Pump 3.	18
Figure 9 Total uncertainty of Pump 3.	18
Figure 10. Time-dependent variability versus instrument uncertainty for Pump 3.	19
Figure 11. Results for Pump 4.	20
Figure 12. Total uncertainty of Pump 4.	20
Figure 13. Time-dependent variability versus instrument uncertainty for Pump 4.	21
Figure 14. Results for Pump 5.	22
Figure 15. Total uncertainty of Pump 5.	22
Figure 16. Time-dependent variability versus instrument uncertainty for Pump 5.	23
Figure 17. Relative uncertainties associated with Pump 3 with curve fits.	24
Figure 18. Relative uncertainties associated with Pump 4 with curve fits.	24
Figure 19. Relative uncertainties associated with Pump 5 with curve fits.	25
Figure 20. Results for V1, V3, V6, and V7.	26
Figure 21. Results for V8, V9, V10, V11, V12, and V13.....	27
Figure 22. Total uncertainty for V1, V3, V6, V7, V8, and V9.....	28
Figure 23. Total uncertainty for V10, V11, V12, and V13.....	29

TABLE OF TABLES

Table 1. Uncertainties of temperature, voltage, and current measurements of DAQ hardware.....	7
Table 2. Instrument uncertainties.....	7
Table 3. Pump 1 Test Matrix	9
Table 4. Pump 2 Test Matrix	9
Table 5. Pump 3 Test Matrix	10
Table 6. Pump 4 Test Matrix	11
Table 7. Pump 5 Test Matrix	11
Table 8. Valve feedback channel numbers.	12
Table 9. Uncertainties for Pump 1 and Pump 2.....	23
Table 10. Curve fits for Pumps 3, 4, and 5.	25
Table 11. Uncertainties for the valves.	29

Nomenclature

ν	degrees of freedom
a	calibration constant
b	intercept
m	slope
s	standard deviation
se	standard error
t	value of the Student t-test
u	uncertainty
x	independent variable
y	dependent variable
AI	analog input
AO	analog output
HX	heat exchanger
IBAL	Intelligent Building Agents Laboratory
J	the number of data points in a single experiment
K	number of days over which an experiment is run
L	number of runs of an experiment on a given day
P	pressure
S	value used in calculating a linear curve fit
S/N	serial number
SS	sum of squares
SS_{Resid}	sum of the square of residuals
Y	value of each data point

Subscripts

0	term in the calibration curve fit
1	level 1 result; term in the calibration curve
2	level 2
li	level 1 result on the i^{th} day
1lk	interim level 1 result
2l	interim level 2 result
cal	calibration
d	downstream
e	expanded
inst	instrument
l..	value of tests over K days
lk.	value of one test on a given day
lkj	individual data point
r	residual
total	calculated from all results
u	upstream
xx	term using only independent variable
xy	term using the independent and dependent variables
R	reproducibility

Other symbols

\bar{x}	mean of “x”
\hat{x}	value of “x” from a curve fit

1. Introduction

The Intelligent Building Agents Laboratory (IBAL) has been designed and constructed as a testbed for the evaluation and design of intelligent control algorithms. The facility is designed to emulate a small commercial building and is divided into an air system and a water (hydronic) system. Within the air system, cooling load are generated by Zone Simulators, which contain electric heating elements and steam spray humidifiers. The Zone Simulators emulate the zones that exist in a real building. Standard commercial air conditioning equipment, including air handling and variable air volume units, supply cold air to the Zone Simulators. The hydronic system consists of chillers, a water side economizer (WSE), and a thermal storage tank that produces cold propylene glycol for the cooling coils in the air handling units. Each pump and fan in the system is operated using a variable frequency drive (VFD). The hydronic side of the system is depicted in Figure 1 and was fully described in TN1933 [1]. The laboratory contains nearly 300 input and output data channels.

Each sensor in the IBAL has a measurement uncertainty due to contributions from sources including calibration, data acquisition, and time-dependent effects. TN1933 discussed calibration and data acquisition uncertainty in detail, and some of that information is duplicated in this document. Additional sensors have also been installed or re-located since that publication, so that information is updated as needed. The primary purpose of this document is to describe the method of assessing time-dependent effects and combining all the uncertainty components into a single value for each sensor in the hydronic system. Figure 1 shows the major components in the hydronic system. Flow rate, upstream and downstream pressure, and power consumption are the key values measured for each of the five pumps. The valve position is the key value measured for the 10 valves.

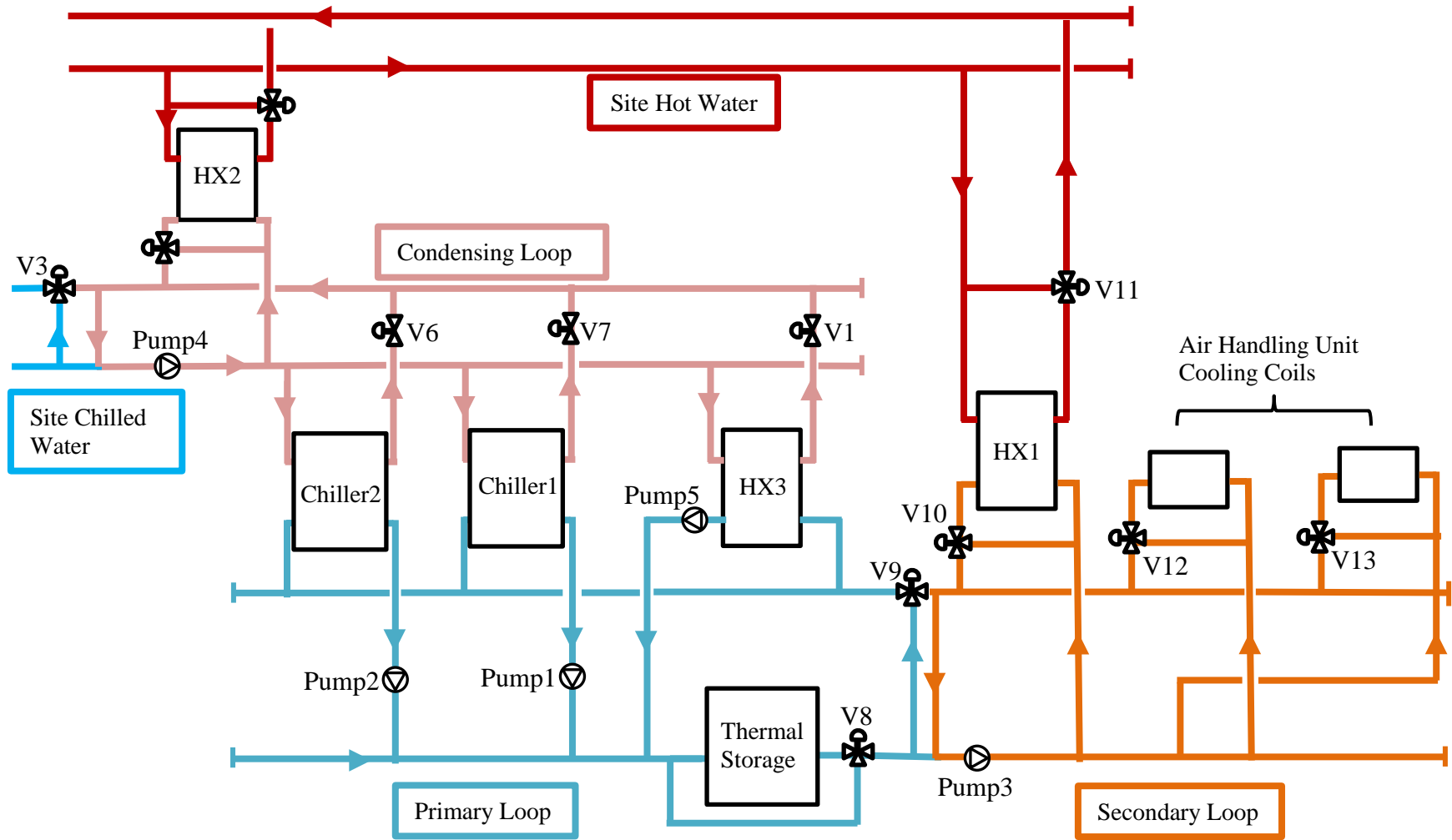


Figure 1. Schematic of the IBAL hydronic system. HX3 is the water side economizer

2. Uncertainty Calculations

This section discusses the methods for calculating individual components of measurement uncertainty and the combination of those components into a single value. Some of the information has been adapted from TN1933 [1]. The measurement variables that these methods are applied to include: flow rate, pressure, and power.

2.1. Time-Dependent Variability

Chapter 2.4.4 of the *Engineering Statistics Handbook* [2] defines three levels of time-dependent variability:

- 1) Level 1 – repeatability or short term variability
- 2) Level 2 – reproducibility or day-to-day variability
- 3) Level 3 – stability or run-to-run variability

As stated in the *Engineering Statistics Handbook*, the first two levels of variability are generally sufficient, so the IBAL calculations only evaluate Level 1 and Level 2 variability. In the following equations, J is the number of repetitions of a measurement acquired during a single experiment, K is the number of days over which the same experiment is executed (reproduced), and L is the number of runs of an experiment on a given day. In all of the experiments discussed here, L = 1 (i.e., Level 3 variability is neglected).

Level 1 is the repeatability standard deviation, and the first step is to calculate the standard deviation of the J measurements, s_{1lk} , during a single test run as shown in Eq. (1). The value of each data point is Y_{lkj} and the mean of the J data points is $\bar{Y}_{lk.}$ (Eq. (2)).

$$s_{1lk} = \sqrt{\frac{1}{J-1} \sum_{j=1}^J (Y_{lkj} - \bar{Y}_{lk.})^2} \quad (1)$$

$$\bar{Y}_{lk.} = \frac{1}{J} \sum_{j=1}^J Y_{lkj} \quad (2)$$

The pooled repeatability standard deviation, s_l , is calculated from the individual standard deviations in order to estimate the standard deviation of the entire data set. The first step is to use Eq. (3) to calculate the sum of squares of the individual standard deviations. When L = 1, there is a single value of s_{1lk} for each of the K days, so s_{li} is the standard deviation of the i^{th} day and v_i is the degrees of freedom (J – 1) of the i^{th} day. The total degrees of freedom for K days is then given in Eq. (4). These parameters are used to calculate the pooled standard deviation as shown in Eq. (5).

$$SS \text{ (Sum of Squares)} = \sum_{i=1}^K \nu_i s_{1i}^2 \quad (3)$$

$$\nu = \sum_{i=1}^K \nu_i \quad (4)$$

$$s_1 = \sqrt{\frac{SS}{\nu}} \quad (5)$$

Level 2 is the reproducibility standard deviation, which is a measure of the day-to-day variability of a measurement. The IBAL will be used to compare the performance of control algorithms under the same set of test conditions on different days. The degree to which the test conditions are the “same” can be quantified by evaluating the day-to-day variability of the key devices in the system. In the hydronic system, these key devices are pumps and valves. The value s_{2l} is calculated from Eq. (6), where $\bar{Y}_{l..}$ is the mean of the daily means ($\bar{Y}_{lk.}$) and is calculated by Eq. (7). Just as in the case of the Level 1 standard deviation, a pooled standard deviation, s_2 , is calculated as shown in Eqs. (8) and (9). The degrees of freedom, ν_i , is the number of days, K , minus one.

$$s_{2l} = \sqrt{\frac{1}{K-1} \sum_{k=1}^K (Y_{lk.} - \bar{Y}_{l..})^2} \quad (6)$$

$$\bar{Y}_{l..} = \frac{1}{K} \sum_{k=1}^K \bar{Y}_{lk.} \quad (7)$$

$$SS \text{ (Sum of Squares)} = \sum_{i=1}^n \nu_i s_{2i}^2 \quad (8)$$

$$s_2 = \sqrt{\frac{SS}{\nu}} \quad (9)$$

These standard deviations are combined to yield the uncertainty of a single measurement, s_R , as shown in Eq. (10). If the Level 3 variability was considered it would also be included in this equation.

$$s_R = \sqrt{\frac{K-1}{K} s_2^2 + \frac{J-1}{J} s_1^2} \quad (10)$$

2.2. Uncertainty of the Calibration Curve Fit [1]

This section contains the equations used to calculate the uncertainty of the curve fit derived from calibration data that relates the measured current or voltage signal to the engineering units of the sensor. In the case of pressure transducers, voltage is converted to kPa (psi) and in the case of flow meters, current is converted to m³/h (gpm). For both sensor types the relationship between the measured signal and engineering units is linear. During calibration, pressure or flow is the independent x variable, while the voltage or current is the dependent y variable. Eq. (11) shows the relationship between the dependent and independent variables, where the slope m and intercept b are found from the calibration data as shown in Eqs. (12) and (13) [3].

$$y = mx + b \quad (11)$$

$$m = \frac{S_{xy}}{S_{xx}} \quad (12)$$

$$b = \bar{y} - m\bar{x} \quad (13)$$

$$\bar{x} = \frac{\sum_{i=1}^n x_i}{n} \quad (14)$$

$$S_{xy} = \sum x_i y_i - \frac{\sum x_i \sum y_i}{n} = \sum (x_i - \bar{x})(y_i - \bar{y}) \quad (15)$$

$$S_{xx} = \sum x_i^2 - \frac{(\sum x_i)^2}{n} = \sum (x_i - \bar{x})^2 \quad (16)$$

The standard error of the calibration is determined from the fit by first calculating the residual y_r between the fit \hat{y} and the measured y as shown in Eqs. (17) and (18).

$$\hat{y} = mx + b \quad (17)$$

$$y_r = y - \hat{y} \quad (18)$$

The standard error, se , is calculated by dividing the sum of the squares of the residuals, SS_{Resid} , by the number of degrees of freedom, ν , and taking the square root. The expanded

standard error, se_e , is the 95 % confidence interval and is calculated by multiplying the se by the t -statistic that corresponds to the degrees of freedom. See Eqs. (19) through (22). This final error is the calibration uncertainty.

$$SSResid = \sum_{i=1}^n y_{r_i}^2 \quad (19)$$

$$\nu = n - 2 \quad (20)$$

$$se = \sqrt{\frac{SSResid}{\nu}} \quad (21)$$

$$se_e = t \cdot se \quad (22)$$

In order to apply the calibration curve fit to experimental data, in which voltage or current is now the independent variable, the relationship defined by Eq. (11) has to be rewritten as shown in Eq. (23) to solve for the engineering units.

$$x = \frac{y - b}{m} \quad (23)$$

The slope and intercept used in the software, a_1 and a_0 , respectively, are derived from Eq. (23) and shown in Eq. (24). In the LabVIEW program, the measured voltage, for example, is converted to engineering units of psi for use in calculations and monitoring.

$$a_0 = -\frac{b}{m}, \quad a_1 = \frac{1}{m} \quad (24)$$

The uncertainty also has to be scaled, but this occurs after all of the components of uncertainty have been combined.

2.3. Uncertainty of Data Acquisition Equipment

Table 1 lists the uncertainties specified by the manufacturer of each data acquisition (DAQ) card. AI is analog input and AO is analog output. The total instrument uncertainty, u_{inst} , includes the calibration uncertainty and the uncertainty of the DAQ hardware, and is given in Table 2 for each instrument evaluated in this study. The Channel is the assigned channel number of the measurement.

Table 1. Uncertainties of temperature, voltage, and current measurements of DAQ hardware.

DAQ Card	AI uncertainty	Units	AO uncertainty	Units
A	0.126	°C		
B	0.002460	V		
C	0.0000188	A	0.0000523	A
D	0.00166	V	0.00189	V
E			0.00107	V
			0.000000448	A
F	0.001520	V	0.00189	V

Table 2. Instrument uncertainties.

Component	Sensor	Channel	u_{inst}
Pump 1	Flow Rate	193	0.14 m ³ /hr (0.6 gpm)
	Upstream Pressure	19	2.9 kPa (0.42 psi)
	Downstream Pressure	20	6 kPa (0.87 psi)
	Power Consumption	54	2.47 W
	Head		6.7 kPa (0.97 psi)
Pump 2	Flow Rate	195	0.13 m ³ /hr (0.57 gpm)
	Upstream Pressure	27	3.9 kPa (0.57 psi)
	Downstream Pressure	28	4.2 kPa (0.61 psi)
	Power Consumption	55	2.47 W
	Head		5.7 kPa (0.83 psi)
Pump 3	Flow Rate		0.34 m ³ /hr (1.48 gpm)
	Upstream Pressure	29	3.7 kPa (0.53 psi)
	Downstream Pressure	30	2.9 kPa (0.42 psi)
	Power Consumption	56	2.47 W
	Head		4.7 kPa (0.68 psi)
Pump 4	Flow Rate		1 % of reading
	Upstream Pressure	31	3.7 kPa (0.54 psi)
	Downstream Pressure	32	2.9 kPa (0.42 psi)
	Power Consumption	57	2.47 W
	Head		4.7 kPa (0.68 psi)
Pump 5	Flow Rate		0.14 m ³ /hr (0.61 gpm)
	Upstream Pressure	33	3.7 kPa (0.53 psi)
	Downstream Pressure	34	2.2 kPa (0.32 psi)
	Power Consumption	58	2.47 W
	Head		4.3 kPa (0.62 psi)
V1	Feedback	357	0.00166 V
V3	Feedback	358	0.00166 V
V6	Feedback	377	0.00166 V
V7	Feedback	378	0.00166 V
V8	Feedback	381	0.00166 V
V9	Feedback	382	0.00166 V
V10	Feedback	379	0.00166 V
V11	Feedback	380	0.00166 V
V12	Feedback	383	0.00166 V
V13	Feedback	384	0.00166 V

2.4. Combining Uncertainties

There are two categories of equipment in the hydronic system whose repeatability and reproducibility are important: pumps and valves. For the pumps, the key instrumentation are power meters, pressure transducers, and flow meters. For the power meters, the measurement uncertainty of DAQ Card B, u_V , is 0.00246 V (Table 1). This voltage measurement ($V_{measured}$) is converted to engineering units of W using Eqs. (25) - (27), where $a_0 = - 1000$ W and $a_1 = 1004.016$ W/V (Note: when power is zero the meter outputs 0.996 V). u_W is the instrument uncertainty of the power meters in Table 2.

$$Power = a_0 + a_1 V_{measured} \quad (25)$$

$$\frac{\partial Power}{\partial V_{measured}} = a_1 \quad (26)$$

$$u_W = \sqrt{a_1^2 u_V^2} = 2.47 \text{ W} \quad (27)$$

For the pumps, the key value is the head, which is the difference between the upstream, P_u , and downstream, P_d , pressure measurements. The uncertainty of the head is calculated using Eqs. (28) - (31).

$$\Delta P = P_d - P_u \quad (28)$$

$$\frac{\partial \Delta P}{\partial P_d} = 1 \quad (29)$$

$$\frac{\partial \Delta P}{\partial P_u} = -1 \quad (30)$$

$$u_{\Delta P} = \sqrt{(1)^2 u_{P_d}^2 + (-1)^2 u_{P_u}^2} \quad (31)$$

The total uncertainty, accounting for instrument uncertainty and Level 1 and Level 2 uncertainties is calculated using Eq. (32). This uncertainty has engineering units, but the relative uncertainty in percent can be calculated by dividing the uncertainty by the mean value of the measurement (e.g., divide u_{total} for the head by the mean head for a given test run as described below) and multiplying by 100. If necessary, the uncertainty is scaled to the correct engineering units using Eq. (33), where m is the slope from Eq. (12).

$$u_{total} = \sqrt{u_{inst}^2 + s_R^2} \quad (32)$$

$$u_{cal} = \frac{u_{total}}{m} \quad (33)$$

3. Experimental Design

This section contains a test matrix for each pump and valve in the hydronic system. The test matrices were generated based on the anticipated system operating conditions. The hydronic system operates in a primary-secondary configuration. Pump 1 and Pump 2 in the primary loop operate at a fixed speed and Pump 3 in the secondary loop operates at a variable speed that scales with the load on the system. In general, the flow rate in the secondary loop will be less than the flow rate in the primary loop. Pump 4 is the condensing loop pump and its flow rate can vary as a function of the load placed on the condensing loop by the chillers. In all cases the pump speed is determined by the VFD setting, which ranges from 0 Hz (no flow) to 60 Hz (maximum flow). The valves operate based on a control voltage between 0 and 10 V.

3.1. Pump Test Matrices

Table 3 shows the test matrix for Pump 1. The pump performance is affected by the status of Pump 2, which is plumbed in parallel with Pump 1, as well as the position of V8, which impacts the pressure drop in the system that the pump has to accommodate. As mentioned previously, the WSE will not operate when the chillers operate, so the status of Pump 5 is not considered. This is a 2² factorial test. The two variables are the operating status of Pump 2 (on or off) and the position of V8 (open or closed). The test matrix is shown in Table 3. The test matrix for Pump 2, shown in Table 4.

Table 3. Pump 1 Test Matrix

Run	Pump 2	V8 Position
1	off	closed
2	on	closed
3	off	open
4	on	open

Table 4. Pump 2 Test Matrix

Run	Pump 1	V8 Position
1	off	closed
2	on	closed
3	off	open
4	on	open

Pump 3 is impacted by V10, V12, V13, and the pump frequency in Hz. V10, V12, and V13 are set in the open or closed position. V9, although located very near Pump 3, does not influence the pump's performance because the bridge system hydraulically disconnects the primary and secondary loops. The hydraulic separation allows the two loops to operate with

different flow rates. In practice, the flow rate in the primary loop exceeds the flow rate in the secondary loop [4]. Through testing, it was determined that when Pump 3 operates at approximately 35 Hz, the flow rate in the secondary loop is equal to the flow rate in the primary loop. Therefore, the maximum pump frequency used in this test is 35 Hz, as shown in the test matrix for Pump 3 presented in Table 5. The lowest frequency that the pump can operate at and still produce flow is 15 Hz, which is the minimum pump frequency used in the test. A third frequency, 25 Hz, was selected as the midpoint between 15 Hz and 35 Hz.

Table 5. Pump 3 Test Matrix

Run	V10 Position	V12 Position	V13 Position	Pump 3
1	open	closed	closed	15 Hz
2	closed	open	closed	15 Hz
3	open	open	closed	15 Hz
4	closed	closed	open	15 Hz
5	open	closed	closed	25 Hz
6	closed	open	closed	25 Hz
7	open	open	closed	25 Hz
8	closed	closed	open	25 Hz
9	open	closed	closed	35 Hz
10	closed	open	closed	35 Hz
11	open	open	closed	35 Hz
12	closed	closed	open	35 Hz

Pump 4 is impacted by the positions of V6, V7, and V1, and the pump frequency in Hz. The WSE is plumbed in parallel with the chillers, so there are no conditions when V1 will be open while V6 and/or V7 are open (i.e., the WSE is not in use when either chiller is in use). This pump may operate at its maximum frequency of 60 Hz, so that is one of the three frequencies used in the test. Initially, the minimum frequency was set to 15 Hz, but the pump displayed inconsistent behavior at that frequency and the minimum was changed to 20 Hz. The third speed of 37 Hz is the midpoint between 15 Hz and 60 Hz. The valves are positioned either open or closed. A $2^3 \times 3^1$ full factorial test matrix, requiring 24 runs, was generated using R [5], an open-source software tool for statistical analysis. The R code used to generate the test matrix is:

```
library(AlgDesign)
dat<-gen.factorial(c(2,2,2,3),factors="all")
```

Of the 24 runs, 12 were removed when: 1) V1 is open at the same time as V6 and/or V7, or 2) all three valves are closed. The resulting test matrix is shown in Table 6; it is the size of a half-fractional factorial design.

Table 6. Pump 4 Test Matrix

Run	V6 Position	V7 Position	V1 Position	Pump 4
1	open	closed	closed	20 Hz
2	closed	open	closed	20 Hz
3	open	open	closed	20 Hz
4	closed	closed	open	20 Hz
5	open	closed	closed	37 Hz
6	closed	open	closed	37 Hz
7	open	open	closed	37 Hz
8	closed	closed	open	37 Hz
9	open	closed	closed	60 Hz
10	closed	open	closed	60 Hz
11	open	open	closed	60 Hz
12	closed	closed	open	60 Hz

Pump 5 is impacted by V8 and the pump frequency in Hz. V8 is positioned open or closed and the pump operates at one of three speeds, although it is unknown at this time if it will be operated as a fixed or variable speed pump. The speeds were selected as the minimum possible frequency of 15 Hz, the maximum possible frequency of 60 Hz, and the midpoint of 37 Hz. The test matrix is shown in Table 7.

Table 7. Pump 5 Test Matrix

Run	V8 Position	Pump 5
1	closed	15 Hz
2	open	15 Hz
3	closed	37 Hz
4	open	37 Hz
5	closed	60 Hz
6	open	60 Hz

3.2. Valve Test Matrices

The repeatability and reproducibility of valve position is assessed by randomly actuating the valve multiple times on different days. The feedback signal from each valve is measured at six positions that are set with a control signal of 0 V, 1.5 V, 3.5 V, 5.5 V, 7.5 V, and 9.5 V, in random order. Six positions were selected in order to characterize the valve operation over the full range of possible values. The key measurement parameter for each valve is the feedback signal. Table 8 is a list of the ten valves that are evaluated and the data acquisition feedback channel for each valve.

Table 8. Valve feedback channel numbers.

Valve	Feedback Channel
V1	357
V3	358
V6	377
V7	378
V8	381
V9	382
V10	379
V11	380
V12	383
V13	384

3.3. Complete Test Plan

For every pump and valve, data were collected on at least five different days. For each pump the individual run of each test lasted at least 15 minutes and for each valve the individual run of each test lasted at least 7 minutes. These timeframes were selected so that the system had time to reach steady state and then at least 20 data points could be collected at steady state. Several problems arose during testing. The first day of testing produced questionable results due to programming errors, so those results were thrown out. The first test for Pump 4 was thrown out because the flow meter was set to treat flow rates below 2.3 m³/hr (10 gpm) as zero flow. During the initial data analysis, it was found that the Pump 2 flow rate measurement had excessive variability. Upon further investigation, it was determined that the ultrasonic flow meter, which is clamped around the pipe, had loosened over time and was not firmly clamped to the pipe. This was corrected and replacement tests were conducted.

4. Results

The results for the pumps and valves are presented in this section. In all cases, the uncertainties were calculated using data collected on five different days.

4.1. Pumps

This section presents the results for the five pumps in terms of the mean result for each run of the test matrix defined in Section 3.1, the absolute and relative uncertainties, and the ratio of the time-dependent variability to the instrument uncertainty. A summary of the final total uncertainties that will be used in future tests is included.

4.1.1. Results

Figure 2 shows the mean flow rate, upstream and downstream pressure, power consumption, and pump head for Pump 1 as a function of each run of the test described in Table 3. The error bars are the total uncertainty calculated as described in Section 2. In Run 1, no valves are open and Pump 2 is off; this results in the highest flow rate from Pump 1 and the greatest

power consumption. In Run 2, Pump 2 is turned on, but all the valves are still closed. This results in a reduction in flow rate and power consumption. Pumps 1 and 2 are plumbed in parallel, so when both pumps are in use the total pressure drop across the branch containing Pump 1 must equal the total pressure drop across the parallel branch containing Pump 2. In fact, both pumps operate based on a combined pump curve rather than operating along their own individual pump curves. At design conditions, Pump 1 operates along a flat portion of its pump curve; the head changes very little for a given change in flow rate.

In Run 3, Pump 2 is off and V8 is open, so the propylene glycol can flow through the thermal storage tank. Under this condition, the system pressure increases and the flow rate decreases relative to the case where V8 is closed. When Pump 2 is on and V8 is open, as in the case of Run 4, the flow rate decreases further as the effects combine. The power consumption shows the same trend as the flow rate. The pump upstream and downstream pressures vary from one test run to the next, but the head is relatively constant.

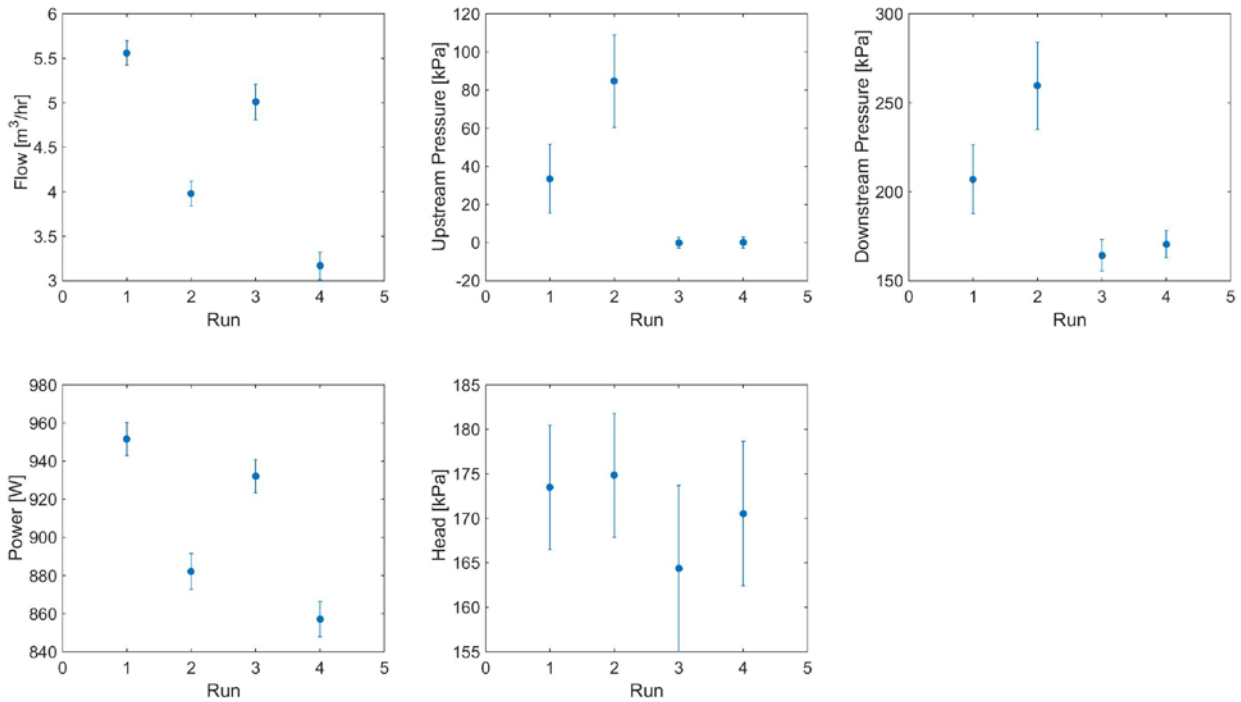


Figure 2. Uncertainty results for each run of the Pump 1 test.

Figure 3 shows the total uncertainty for Pump 1 in both absolute and relative terms. The absolute uncertainty is normalized by the mean measurement and multiplied by 100 % to obtain the relative uncertainty. The absolute uncertainty on the flow rate is less than 0.2 m³/hr (0.9 gpm) for all cases and the relative uncertainty is less than 5 %. The relative uncertainty of the upstream pressure is high and in one case it is so high that the point is not even shown on the figure. Part of the reason for this large uncertainty is that the upstream pressure can be at or near zero, so the relative uncertainty is large. The downstream pressure has an uncertainty of less than 10 %, but the absolute error is similar to the absolute error of the upstream pressure. The downstream pressure is larger, however, so the relative

uncertainty is lower. Interestingly, the uncertainty of the head is lower than the uncertainty of either individual pressure measurement.

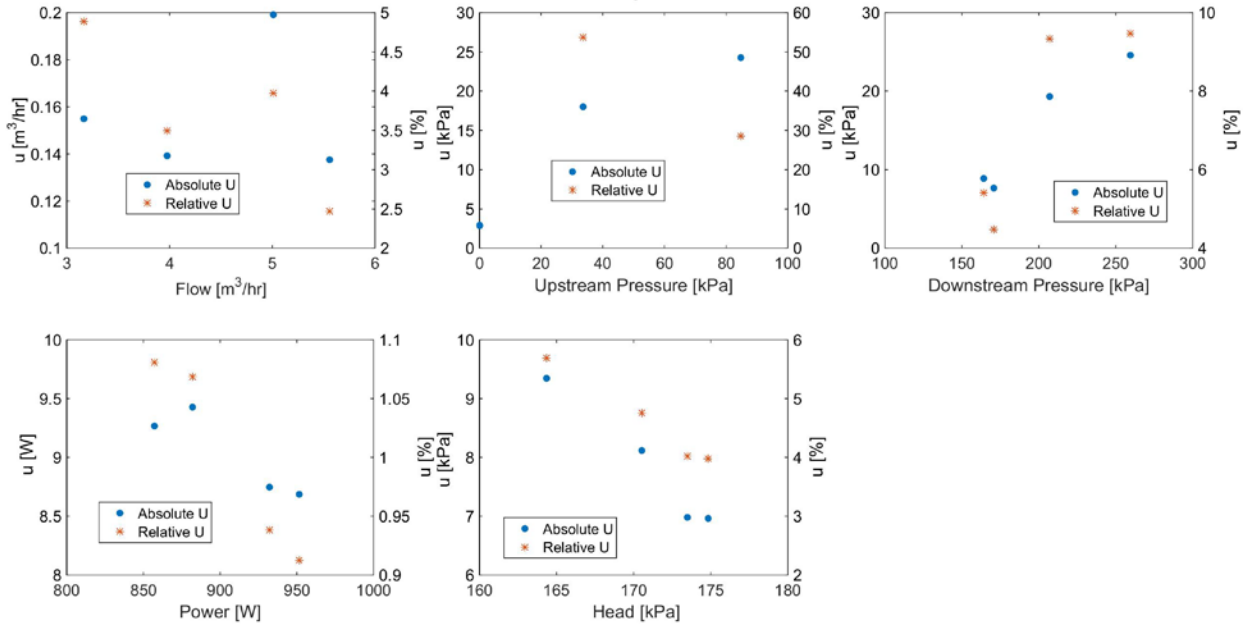


Figure 3. Total uncertainty of Pump 1.

Figure 4 shows the ratio of the time-dependent variability, s_R , to the instrument uncertainty, u_{inst} . A value greater than 1 indicates that the time-dependent variability dominates the instrument uncertainty. The instrument uncertainty is calculated using the individual instrument uncertainties of the upstream and downstream pressure measurements, but the time-dependent variability of the head was calculated by:

1. calculating the head as (downstream pressure – upstream pressure), and
2. calculating s_1 , s_2 , and finally s_R variability of that head.

Although there was substantial variability in the upstream and downstream pressure measurements, that variability was consistent between the two measures and partially canceled out when the head was calculated, so the head shows less time-dependent variability and lower overall uncertainty than either pressure measurement.

For the flow rate, in most cases the ratio of time-dependent variability to the instrument uncertainty is less than one, which indicates that the instrument uncertainty is the primary source of uncertainty. For the upstream pressure, at the lowest pressures the instrument uncertainty is dominant, but at the higher pressures the time-dependent variability is much greater. A similar result is seen in the downstream pressure. One explanation for the high variability is that the pressure transducers are located at the inlet and outlet of the pump, so they are likely to be exposed to turbulent flow. The head, on the other hand, has a greater contribution from the instrument uncertainty, which is consistent with the prior results and is further indication that the cause of the variability in the pressure measurements is consistent in both the upstream and downstream locations. The power consumption is dominated by the time-dependent variability because the instrument uncertainty is very low.

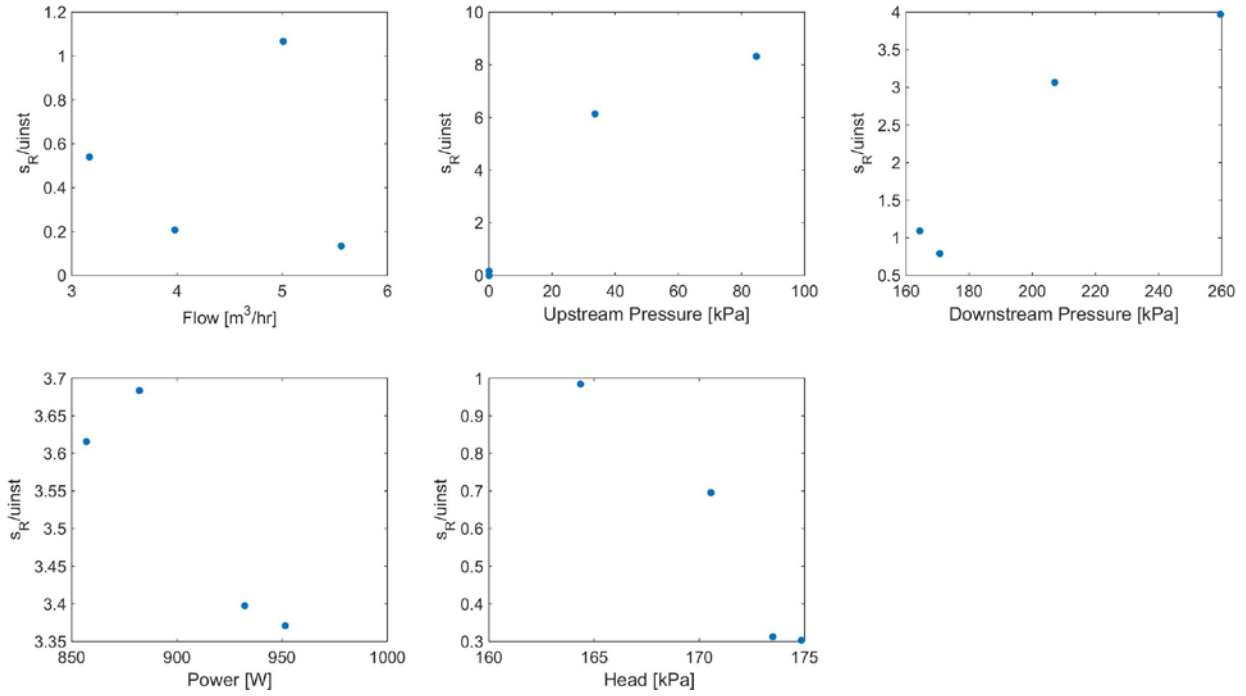


Figure 4. Time-dependent variability versus instrument uncertainty for Pump 1.

Figure 5 shows the uncertainty results for Pump 2 with error bars. As expected, the trends are the same as for Pump 1, though the head changes more because Pump 2 does not operate in the flat portion of its pump curve. Figure 6 shows the uncertainty for the sensors associated with Pump 2. The uncertainties of the power and head measurements are slightly greater than for Pump 1, while the uncertainty of the flow rate measurement is a little lower.

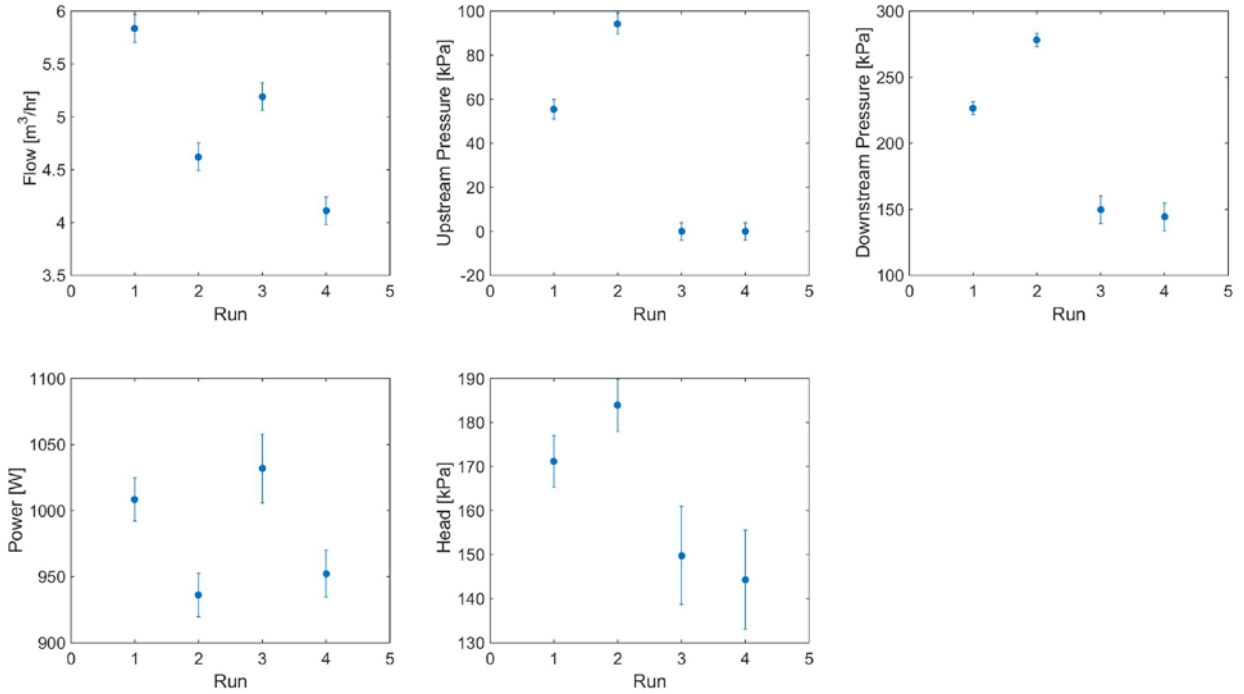


Figure 5. Uncertainty results for each run of the Pump 2 tests.

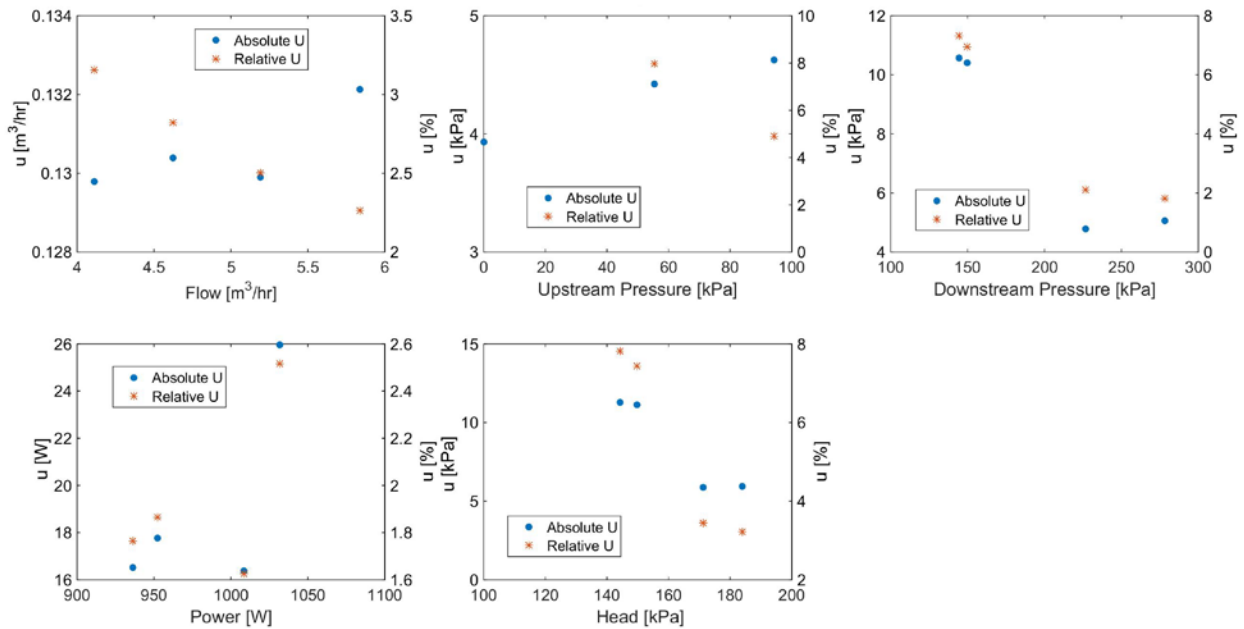


Figure 6. Total uncertainty of Pump 2.

Figure 7 shows the ratio of s_R to instrument uncertainty. The flow rate uncertainty is dominated by the instrument uncertainty, the power measurement is dominated by the time-dependent variability, and the component of uncertainty that dominates the head varies with head; at higher head, the instrument variability dominates. These results are consistent with Pump 1.

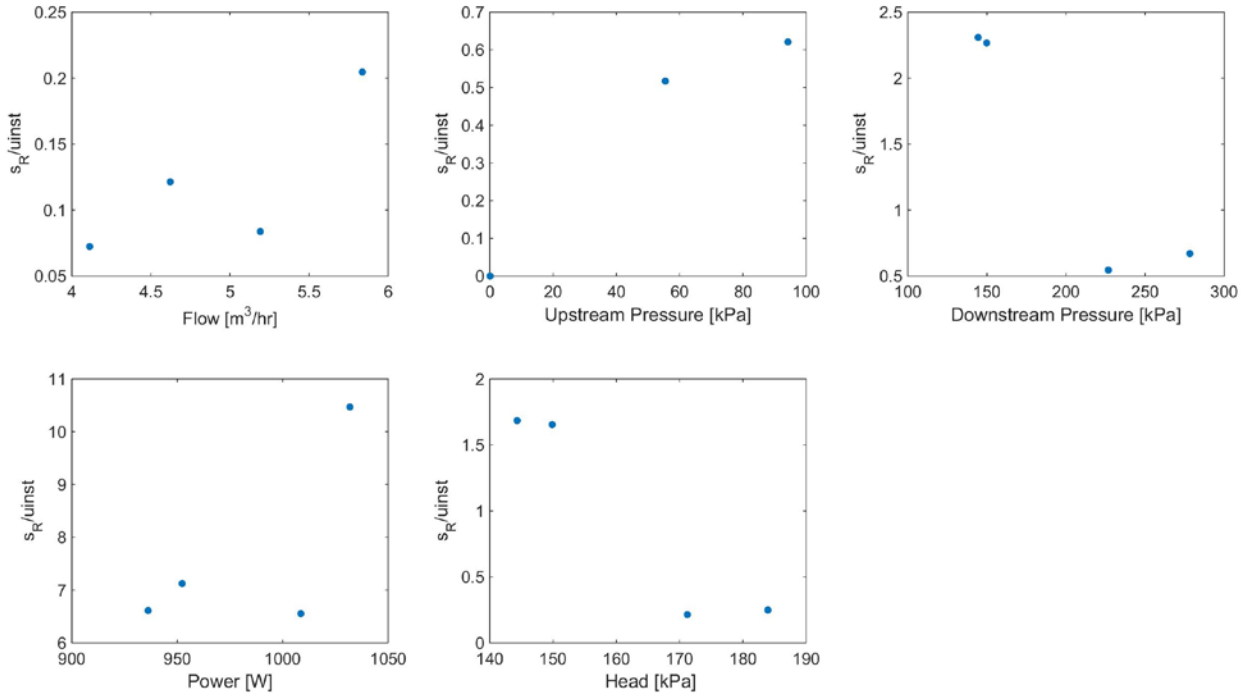


Figure 7. Time-dependent variability versus instrument uncertainty for Pump 2.

The tests for Pump 3 were very different from those for Pump 1 and Pump 2 because it was tested at three different VFD frequencies. The power and head results, shown in Figure 8, trend with frequency: the first four runs are at 15 Hz, the second four runs are at 25 Hz, and the final four runs are at 35 Hz. The flow also trends with pump speed, but the groupings are less apparent because the valve positions also change. V10 has the greatest impact on the pump performance. When the valve is open, as it is in the odd numbered runs, the flow is at its greatest relative to the other runs. V10 is the valve that is closest to the pump and the pipe diameter leading to V10 is larger than that leading to V12 and V13, so when it is open the flow resistance is at its lowest. The bypass legs around the cooling coils are also open all the time, so the system resistance does not change much when V12 or V13 are open for a given position of V10.

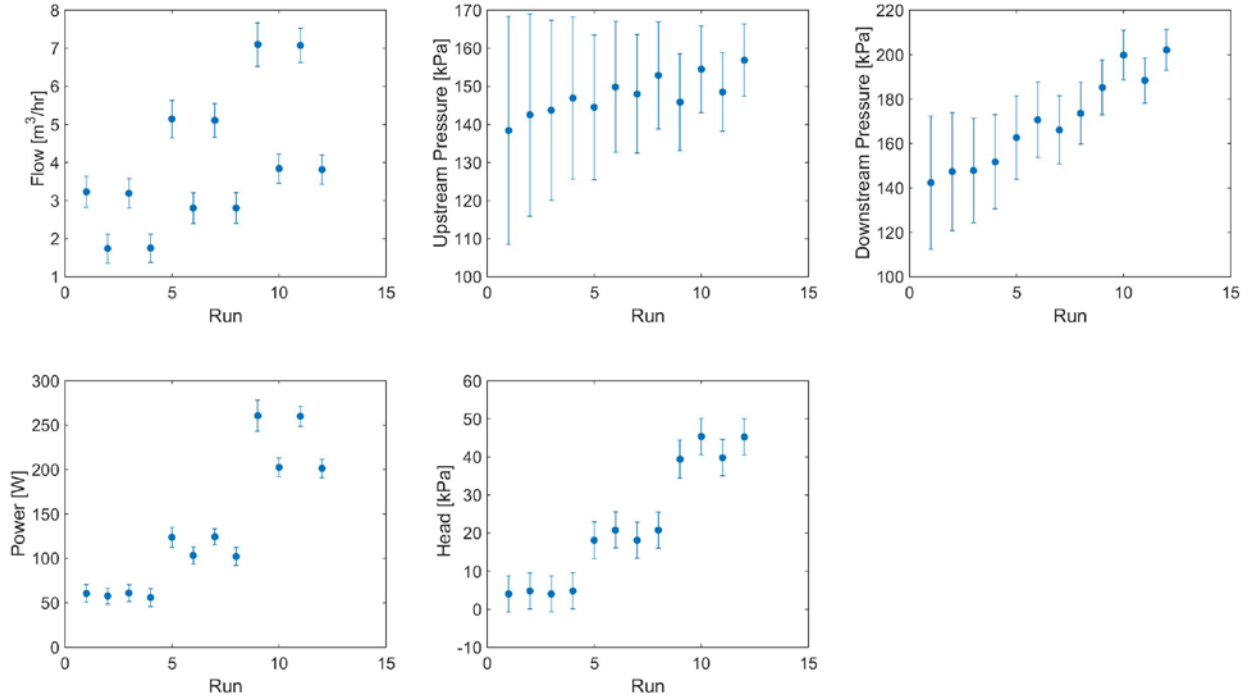


Figure 8. Uncertainty results for each run of the Pump 3 tests.

Figure 9 shows the absolute and relative uncertainties for Pump 3. At lower flow rates, the relative uncertainty is high, but it decreases as flow rate increases. As shown in Figure 10, as the flow rate increases, the time-dependent variability becomes more important. The trend is similar for the power and head measurements, though the opposite trend holds for the individual pressure measurements.

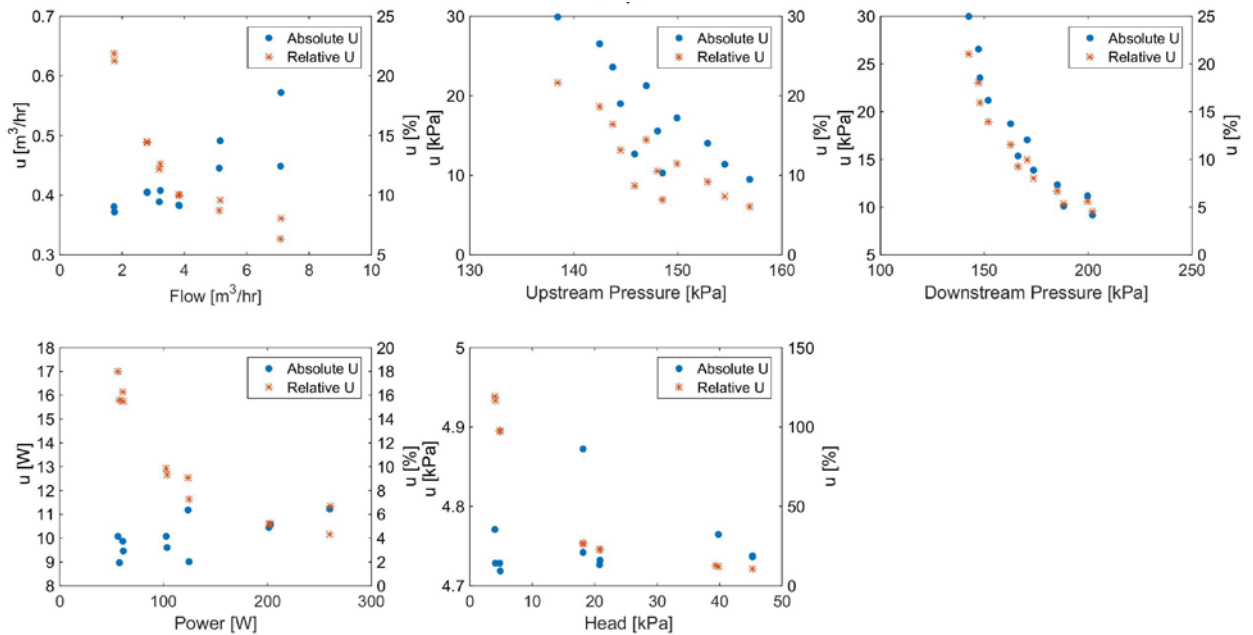


Figure 9 Total uncertainty of Pump 3.

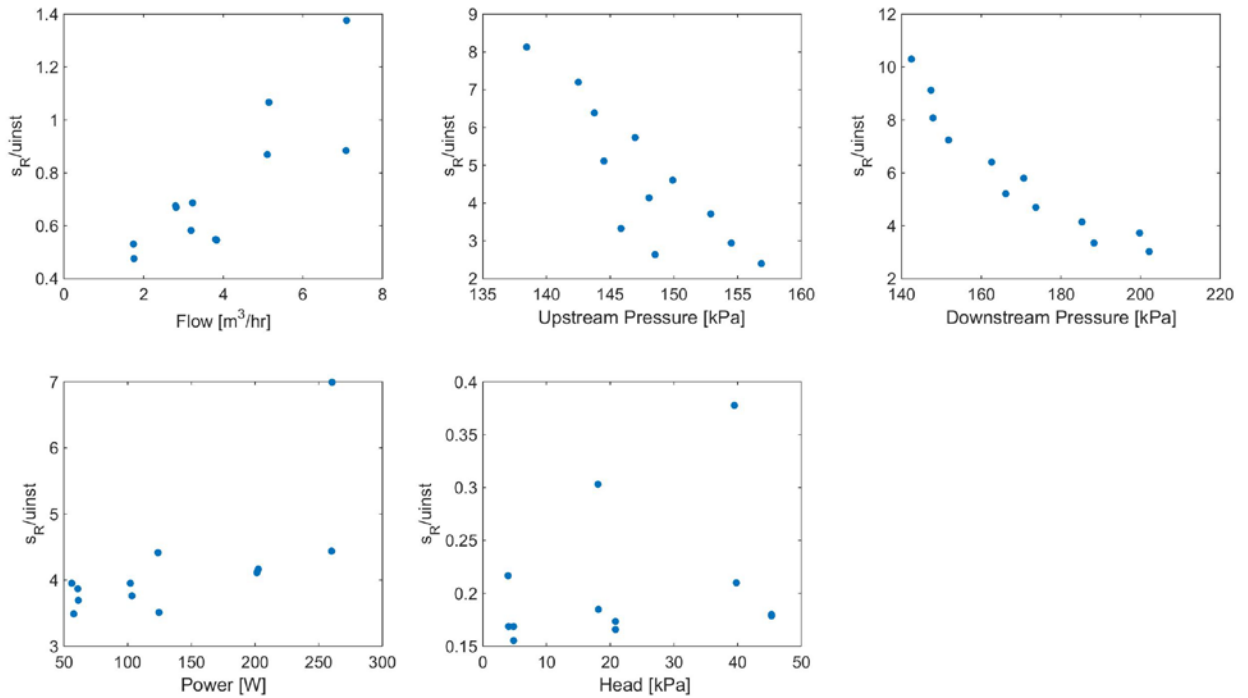


Figure 10. Time-dependent variability versus instrument uncertainty for Pump 3.

Figure 11 and Figure 12 show the results for Pump 4. Pump 4 was also tested at three different VFD frequencies. At the lowest setting of 20 Hz (runs 1 – 4), the relative uncertainties of the flow, power, and head, are higher than at the 37 Hz (runs 5 – 8) and 60 Hz (runs 9 – 12) settings. The flow rate has an uncertainty of less than 10 % at all speeds; the uncertainty of the power and head measurements are less than 10 % at the higher speeds.

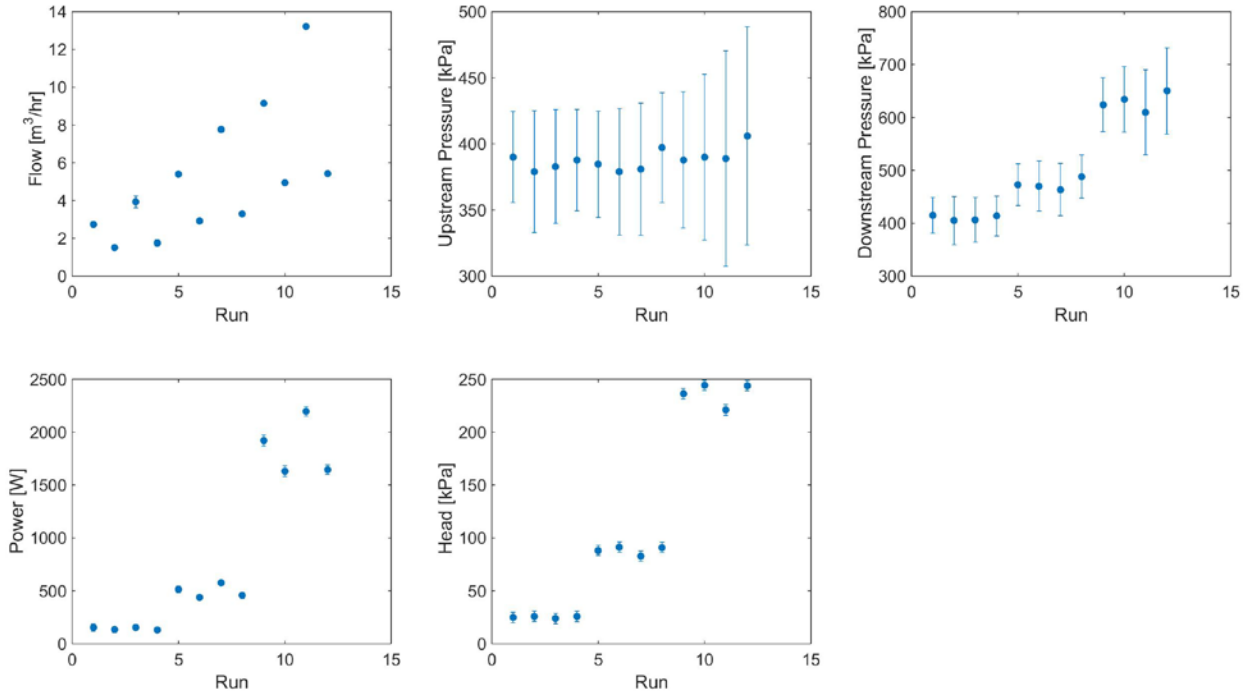


Figure 11. Uncertainty results for each run of the Pump 4 tests.

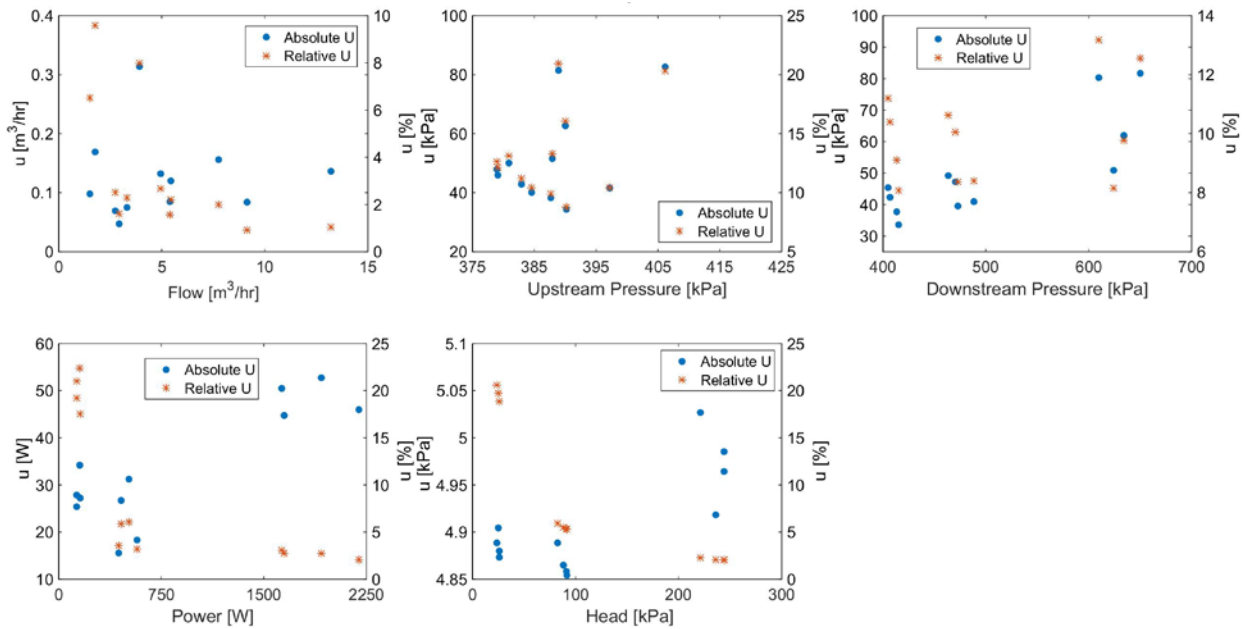


Figure 12. Total uncertainty of Pump 4.

Figure 13 shows the ratio of the time-dependent variability to the instrument uncertainty. Unlike the other pumps, the time-dependent variability dominates the flow rate measurement. The flow meter for Pump 4 is an electromagnetic meter, which is a more accurate measurement of flow than the ultrasonic flow meters used in other locations.

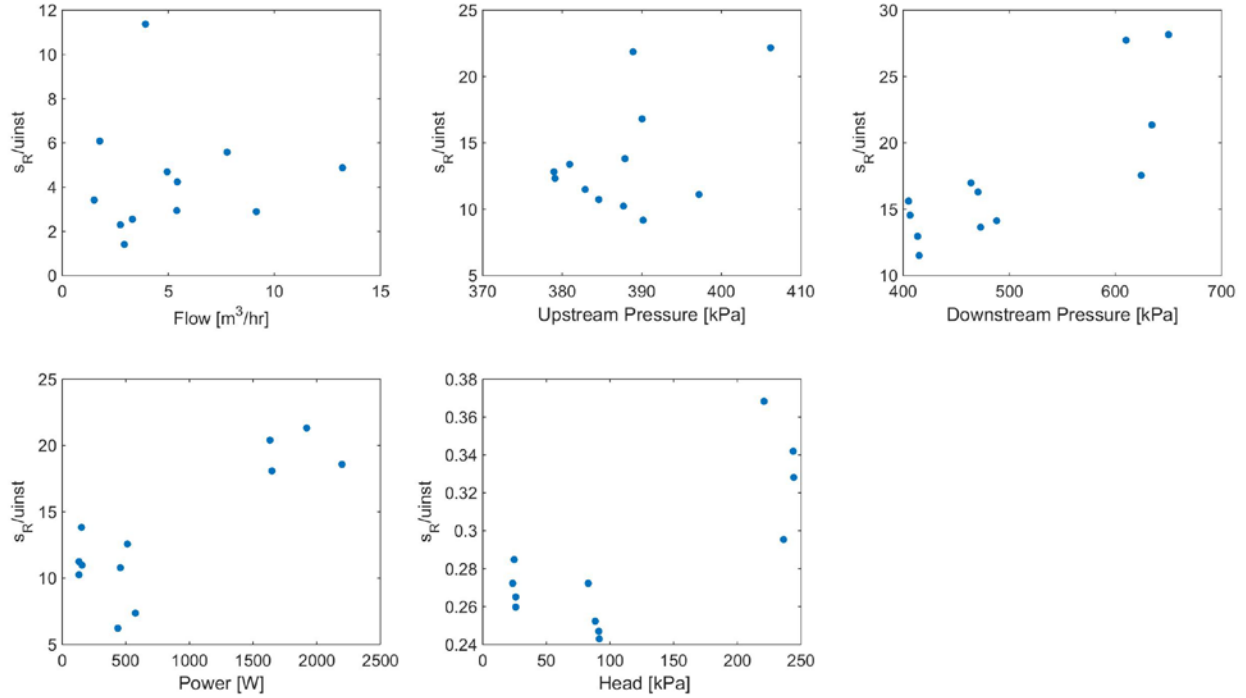


Figure 13. Time-dependent variability versus instrument uncertainty for Pump 4.

Figure 14 shows the results for each run of Pump 5 and Figure 15 shows the absolute and relative uncertainties. Pump 5 was tested at three VFD frequencies and the relative uncertainties are greater than 10 % at the lowest speed (15 Hz, runs 1 and 2). At the higher speeds (runs 3 – 6), the uncertainties are less than 10 %. Figure 16 shows that for the flow rate and head, most of the uncertainty is due to the instrument uncertainty, and most of the uncertainty for the power is the time-dependent variability.

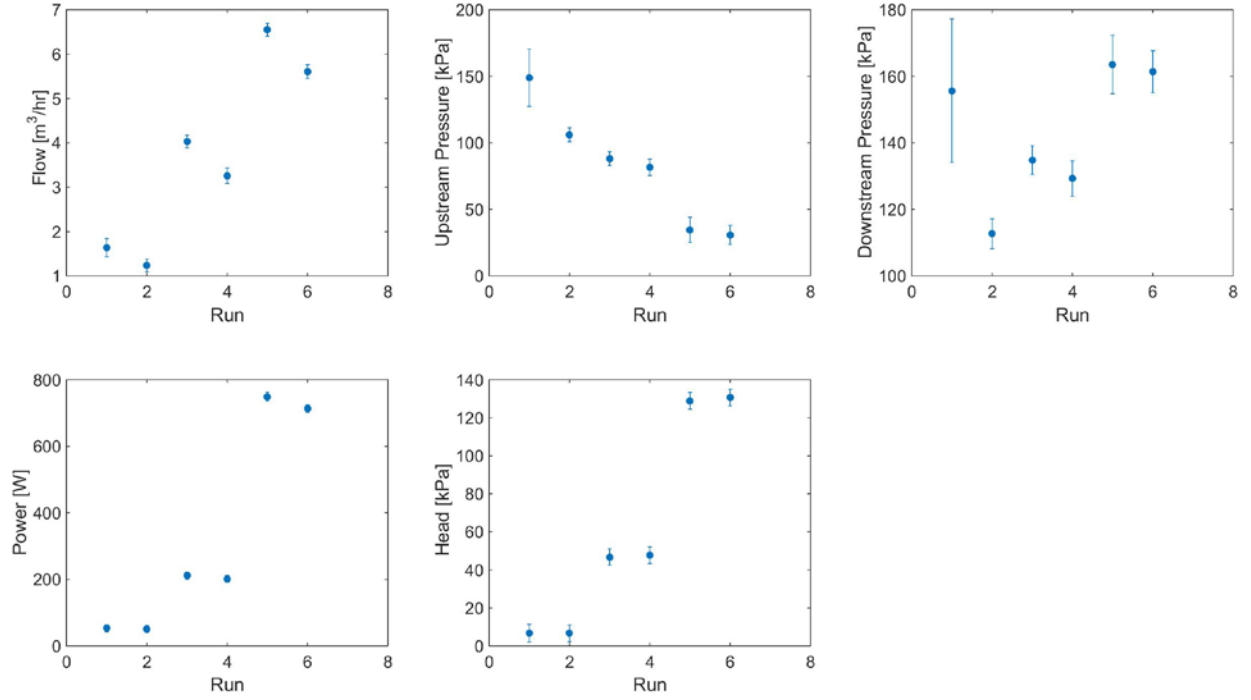


Figure 14. Uncertainty results for each run of the Pump 5 tests.

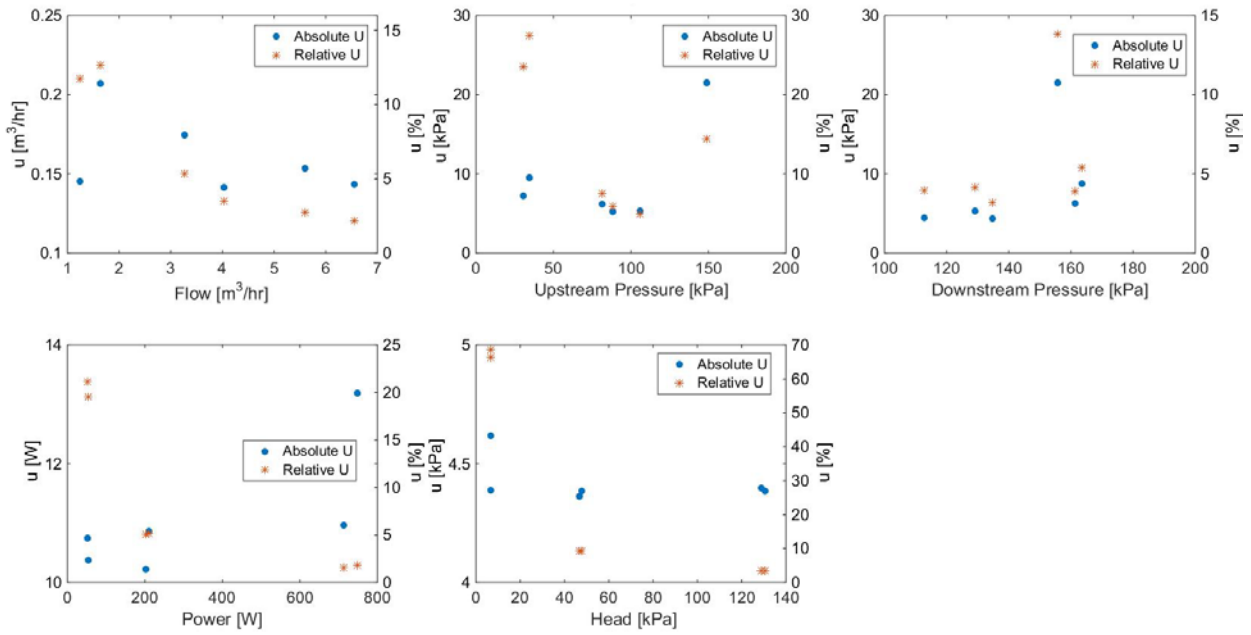


Figure 15. Total uncertainty of Pump 5.

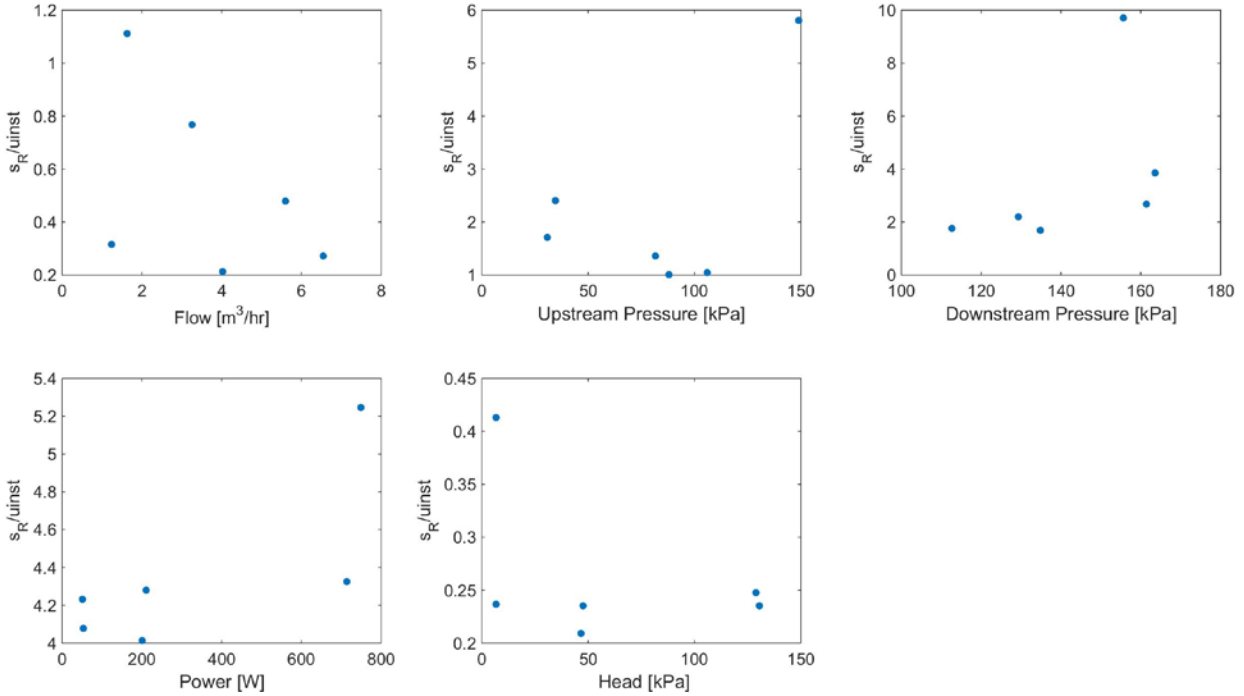


Figure 16. Time-dependent variability versus instrument uncertainty for Pump 5.

4.1.2. Summary

Pumps 1 and 2 operate at 60 Hz and the uncertainty levels are relatively constant for different system configurations (see Figure 3 and Figure 6), so for the instruments used to measure the performance of these pumps a single value of uncertainty, given as a percent of reading, is used, as shown in Table 9. S/N in this table is the serial number of the instrument (see [1] for additional detail).

Table 9. Uncertainties for Pump 1 and Pump 2.

Pump	Measurement	Channel(s)	S/N	Uncertainty
Pump 1	Flow [m ³ /hr]	193	100718	5 %
	Power [W]	54	14090248	1.2 %
	Head [kPa]	19, 20	2058089.29, 2058089.33	6 %
Pump 2	Flow [m ³ /hr]	195	100717	3.5 %
	Power [W]	55	14090245	2.6 %
	Head [kPa]	27, 28	2058089.32, 2058089.31	8 %

Pumps 3, 4, and 5 were tested at different VFD frequencies and the resulting uncertainties showed variation with flow rate, power consumption, and head, so rather than assigning a single value for uncertainty, the uncertainty will be calculated based on a curve fit to the data. Figure 17 through Figure 19 show the relative uncertainty with the curve fits. Note that the data follow a log-log trend, so the curve fits are in terms of the log of the uncertainty and the log of the flow rate, power, or head.

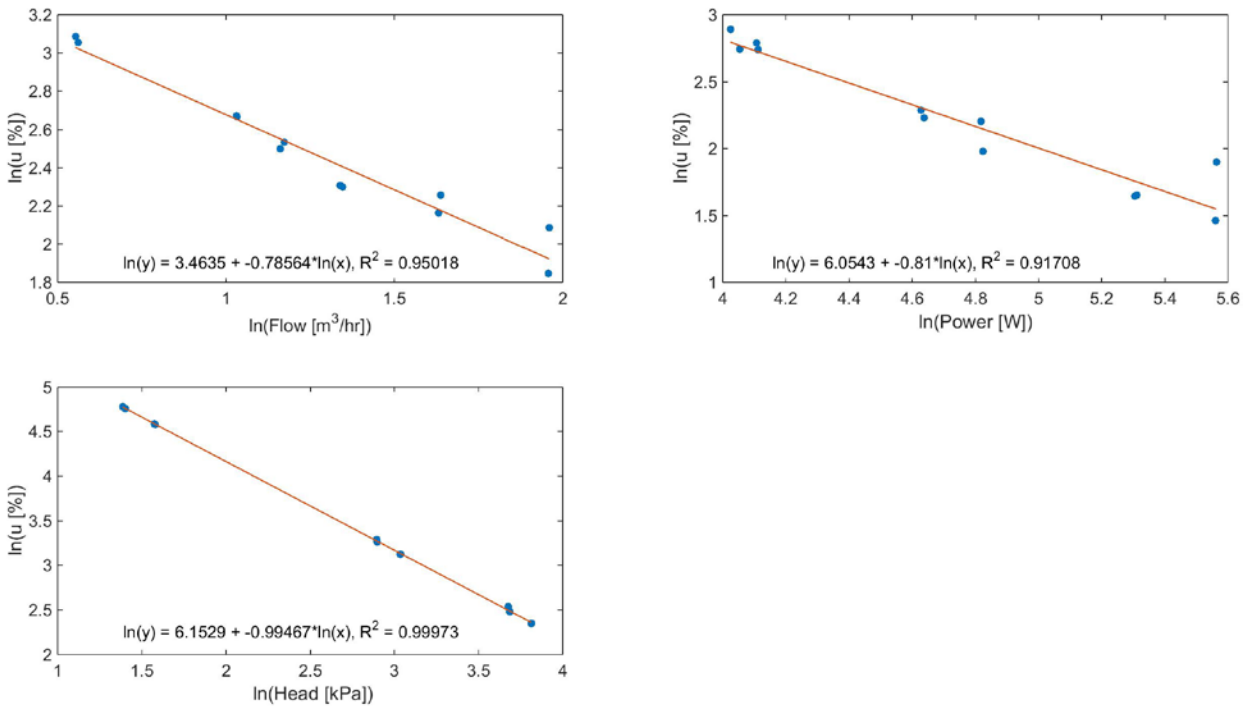


Figure 17. Relative uncertainties associated with Pump 3 with curve fits.

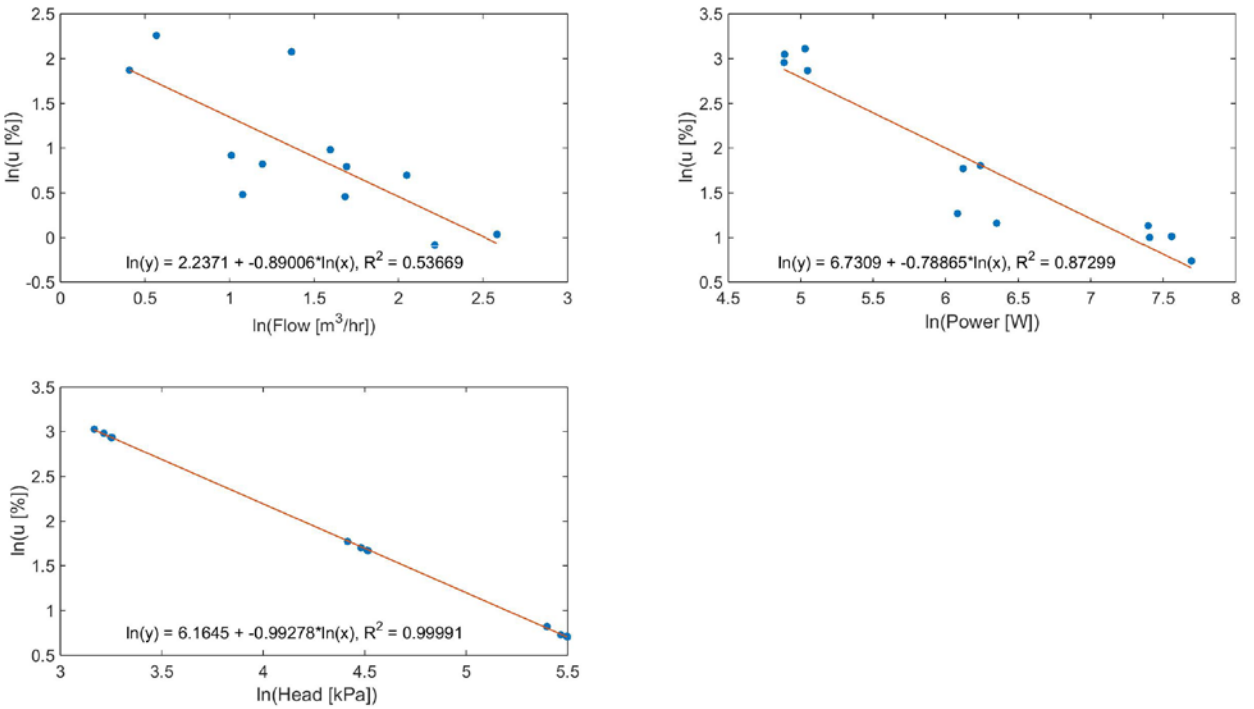


Figure 18. Relative uncertainties associated with Pump 4 with curve fits.

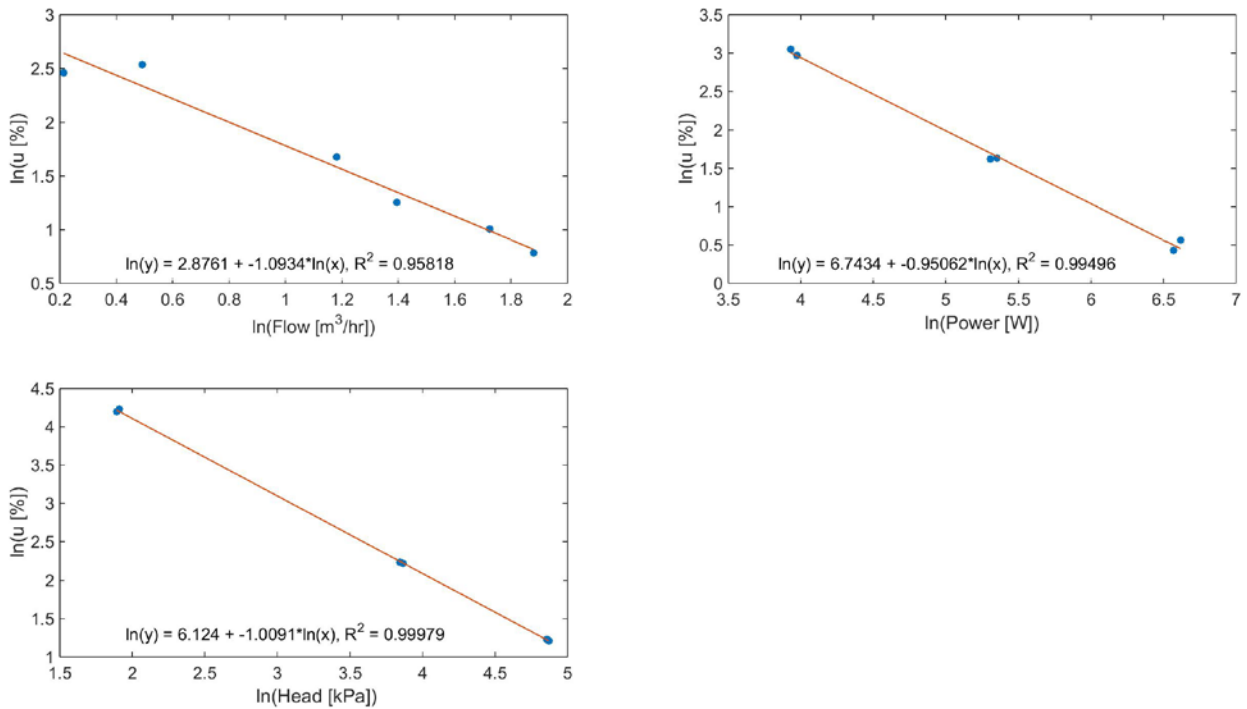


Figure 19. Relative uncertainties associated with Pump 5 with curve fits.

The parameters that define the curve fit described by Eq. (34) are given in Table 10. The fits for Pump 4 are not as good as for the other pumps, particularly at the lowest flow rate.

$$u [\%] = e^{a_0} x^{a_1} \quad (34)$$

Table 10. Curve fits for Pumps 3, 4, and 5.

Pump	x	Channel(s)	S/N	a ₀	a ₁	R ²
P3	Flow [m ³ /hr]	213	100722	3.46	-0.79	0.95
	Power [W]	56	14090237	6.05	-0.81	0.92
	Head [kPa]	29, 30	2058089.25, 071914D101	6.15	-0.99	1.00
P4	Flow [m ³ /hr]	214	FAC1217	2.24	-0.89	0.54
	Power [W]	57	14090244	6.73	-0.79	0.87
	Head [kPa]	31, 32	2058089.27, 2058089.28	6.16	-0.99	1.00
P5	Flow [m ³ /hr]	211	100715	2.88	-1.09	0.96
	Power [W]	58	14090242	6.74	-0.95	0.99
	Head [kPa]	33, 34	2058089.34, 2058089.26	6.12	-1.01	1.00

4.2. Valves

The determination of the valve position uncertainty is much more straightforward than in the case of the pumps because the only factor to consider is the variability of the feedback signal. The variability of the feedback signal becomes important when the valve feedback signal is used by the control system to determine or set the current or future valve positions.

4.2.1. Results

Figure 20 and Figure 21 show the valve feedback signal (position) versus run for each valve. Error bars are included in the plots, though they are so small that they are not visible.

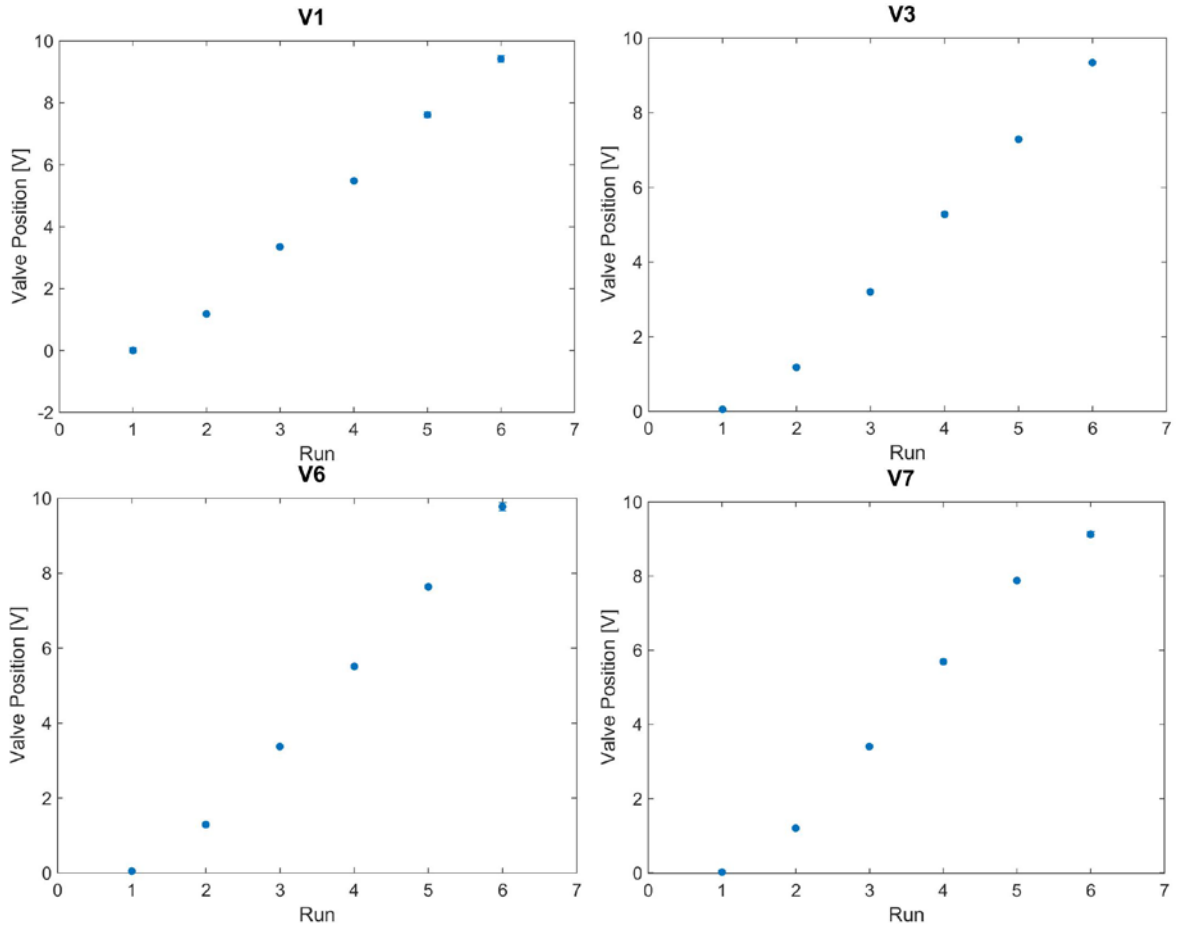


Figure 20. Results for V1, V3, V6, and V7.

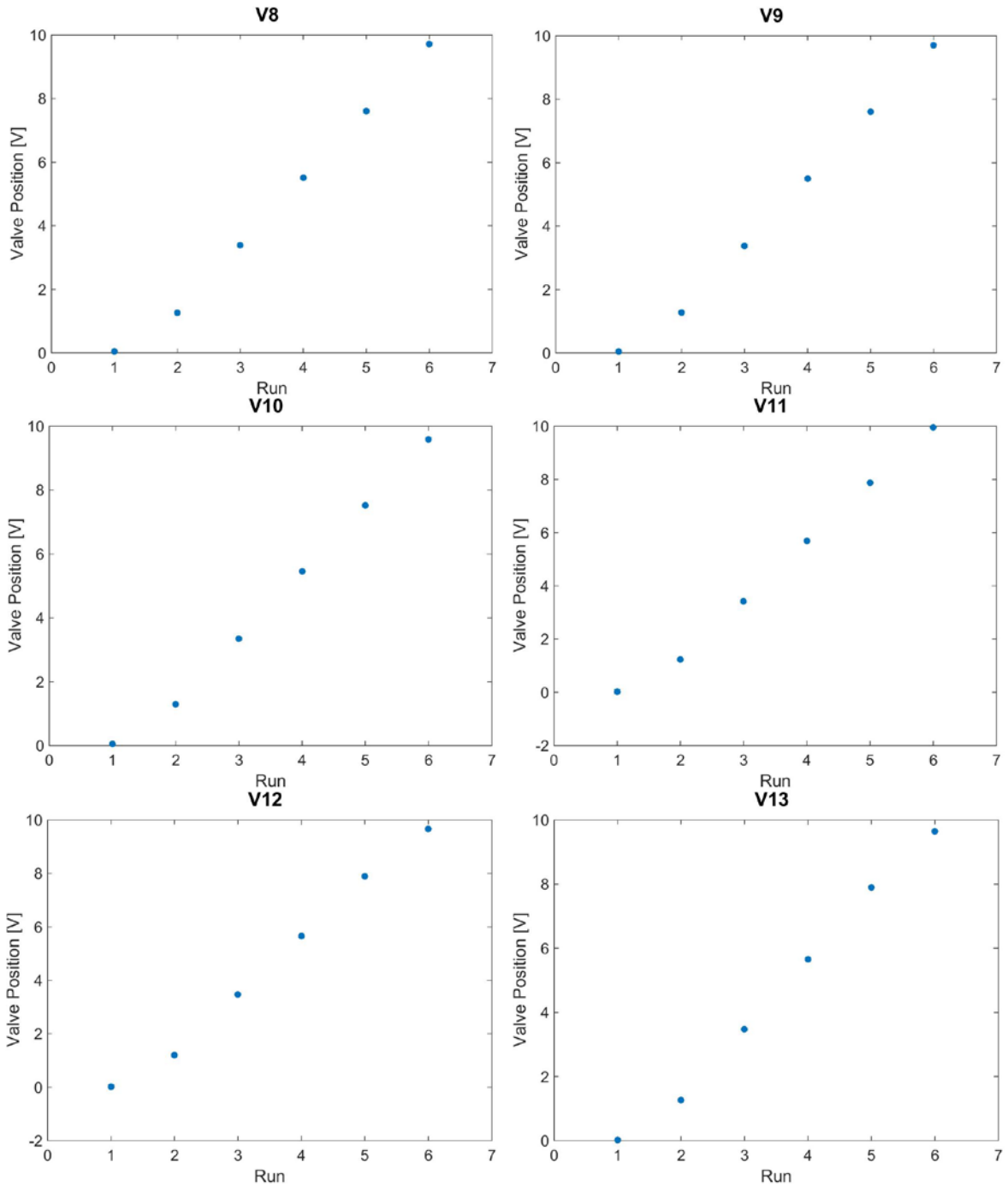


Figure 21. Results for V8, V9, V10, V11, V12, and V13.

Figure 22 and Figure 23 show the total uncertainty for each valve. In general, the uncertainties are less than 0.1 V, but in a few cases the uncertainty is larger. The value of 0.1 V is consistent with prior observation that when the control signal changes by less than 0.1 V, the valve position does not change. For example, if the control signal changes from 4 V to 4.09 V, the feedback signal does not change.

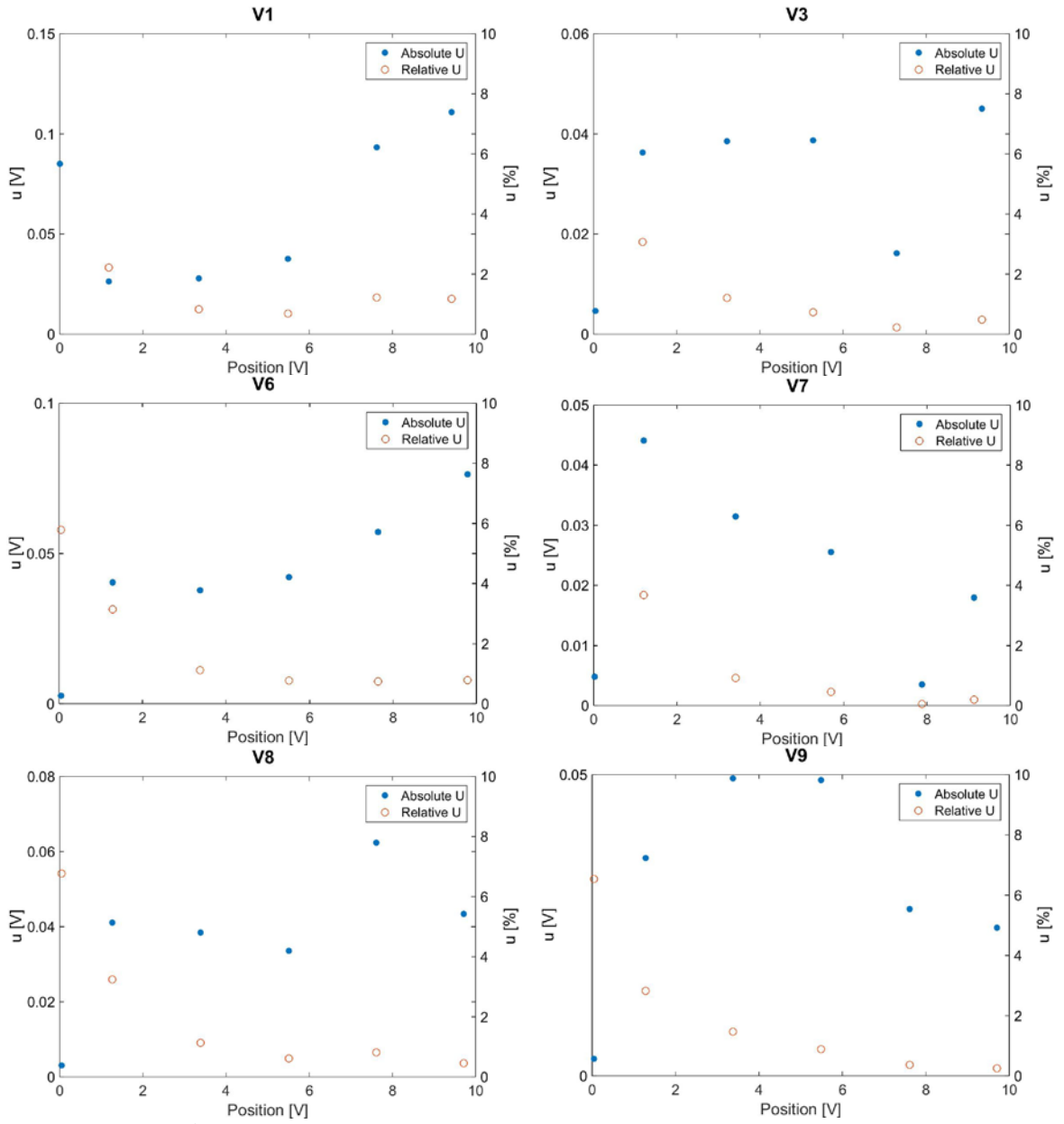


Figure 22. Total uncertainty for V1, V3, V6, V7, V8, and V9.

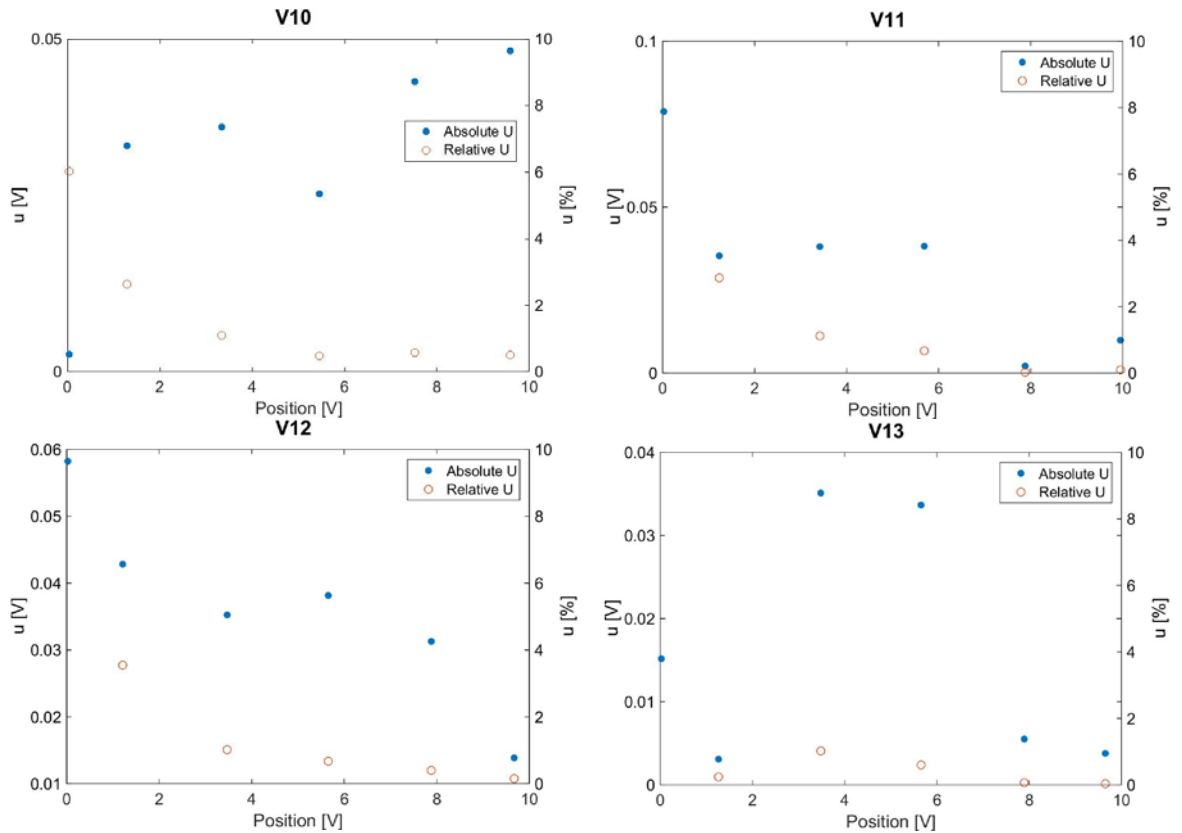


Figure 23. Total uncertainty for V10, V11, V12, and V13.

4.2.2. Summary

The final uncertainty assigned to each valve is given in Table 11.

Table 11. Uncertainties for the valves.

Valve	Channel	P/N	Uncertainty [V]
1	357	Powermite 599	0.11
3	358	Flowrite 599	0.05
6	377	Flowrite 599	0.08
7	378	Powermite 599	0.05
8	381	Flowrite 599	0.07
9	382	Flowrite 599	0.05
10	379	Flowrite 599	0.05
11	380	Powermite 599	0.05
12	383	Powermite 599	0.05
13	384	Powermite 599	0.04

5. Conclusions

This report presented the methods used to determine the total uncertainty of sensors in the hydronic system associated with pumps and valves and are, therefore, impacted by the time-dependent variability of those devices. This method will also be applied in the air system to

account for time-dependent variability in devices such as fans and dampers, which will be described in a future report.

6. References

- [1] A. J. Pertzborn, "Intelligent Building Agents Laboratory: Hydronic System Design," Technical Note 1933, NIST, 2016.
- [2] "NIST/SEMATECH e-Handbook of Statistical Methods," 30 October 2013. [Online]. Available: <http://www.itl.nist.gov/div898/handbook/>. [Accessed 8 May 2017].
- [3] J. Devore and N. Farnum, *Applied Statistics for Engineers and Scientists*, Belmont, CA: Thomson Brooks/Cole, 2005.
- [4] M. A. Reed and C. Davis, "Chilled Water Plant Savings at No Cost," *ASHRAE Journal*, pp. 36-44, June 2007.
- [5] R Core Team, "R: A language and environment for statistical computing," R Foundation for Statistical Computing, 2013.
- [6] U.S. Energy Information Administration, "U.S. Energy Flow, 2015," 2016. [Online]. Available: http://www.eia.gov/totalenergy/data/monthly/pdf/flow/total_energy.pdf. [Accessed 29 August 2016].